Highly efficient, spatially coherent distributed feedback lasers from dense colloidal quantum dot films

Dang, Cuong; Lee, Joonhee; Roh, Kwangdong; Kim, Hanbit; Ahn, Sungmo; Jeon, Heonsu; Breen, Craig; Steekel, Jonathan S.; Coe-Sullivan, Seth; Nurmikko, Arto

2013

Dang, C., Lee, J., Roh, K., Kim, H., Ahn, S., Jeon, H., et al. (2013). Highly efficient, spatially coherent distributed feedback lasers from dense colloidal quantum dot films. Applied Physics Letters, 103, 171104-.

https://hdl.handle.net/10356/79635

https://doi.org/10.1063/1.4826147

Highly Efficient, Spatially Coherent Distributed Feedback Lasers from Dense Colloidal Quantum Dot Films

Cuong Dang,[1] Joonhee Lee,[1] Kwangdong Roh,[2] Hanbit Kim,[3] Sungmo Ahn,[3] Heonsu Jeon,[3] Craig Breen,[4] Jonathan S. Steckel,[4] Seth Coe-Sullivan,[4] and Arto Nurmikko,[1,2*]

[1]School of Engineering, Brown University, Providence, Rhode Island 02912, USA

[2]Department of Physics, Brown University, Providence, Rhode Island 02912, USA

[3]Department of Physics and Astronomy, Seoul National University, Seoul 151-747, Republic of Korea

[4]QD Vision Inc., 29 Hartwell Avenue, Lexington, Massachusetts, 02421, USA

Colloidal quantum dots (CQD) are now making their entry to full-color displays, endowed by their brightness and single-material base. By contrast, many obstacles have been encountered in their use towards lasers. We demonstrate here optically pumped distributed feedback (DFB) lasers, based on close-packed, solid films self-assembled from type-I CQDs. Notably, the single mode CQD-DFB lasers could reach such a low threshold as to be pumpable with a compact pulsed source in a quasi-continuous wave (CW) regime. Our results show the spatially and temporally coherent laser beam outputs with power of 400 μW and a quantum efficiency of 32%.

Semiconductor lasers, based on single crystal epitaxial inorganic semiconductor heterostructures, are versatile and technologically mature. For broad spectrum applications across the visible at red, green, and blue, however, current technology requires at least three different materials, each

with specific device process approaches.[1] By contrast, CQD with their size tailored exciton quantum confinement offer a wide range of color tunability without changing material composition during their common chemical synthesis.[2,3] Endowed by their brightness, the single-material CdSe-based CQDs have now been commercialized for use in full-color displays[4] and bio-labels,[5,6] with considerable ongoing research into quantum light emitters,[7] light emitting diodes,[8-11] and lasers.[12-16] However, progress in laser research has been slow and severely hindered by a fundamental obstacle related to the exciton dynamics in highly excited CQDs, as described below. Furthermore, the inability to created highly-homogeneous, low-loss solid films has made CQDs transition to anywhere near the material quality required in a semiconductor laser difficult. Consequently, studies even if only on the basic attributes of optical gain and stimulated emission in CQDs have been mainly limited to employing ultrashort (sub-picosecond) pulsed[15-18] or impractically high-power longer (>psec) pulsed[19] optical pumping sources. On the device approach, the DFB-type resonators were employed for CQD-based laser structures[16-19] but the impractical pump sources and limited performance are the major problems for applications. By this letter, we show major material and device advances for the prospects of CQDs towards laser reality. Specifically, by integrating the high-performance single-exciton-gain from our novel CQD film into compact DFB laser structures, we have been able to operate the high performance lasers in the quasi-CW regime in the red. The approach is scalable and extendable to reach both green and blue laser colors on a large area for lighting and display applications.

The type-I CQDs with nominal CdSe core diameter of 4.2 nm were prepared by high-temperature organometallic synthesis. The thin (1 nm) ternary shell, $Zn_{0.5}Cd_{0.5}S$, reduces strain and creates a sufficient core/shell bandgap difference (~1.3 eV in bulk-equivalent materials) for electron-hole confinement. The optimum Cd composition provides maximum alloy potential

fluctuations, which lead to spatial localization of exciton wave functions in single II–VI crystals.[20] The CQDs were finally protected by a monolayer of robust aromatic ligands. The CQDs demonstrated a quantum yield exceeding 80% at the high concentrations in a starting solution (up to 150 mg/ml with Toluene solvent). The absolute quantum yield was measured by an integrating sphere with a blue LED as an excitation source. The transient photoluminescence (PL) showed that the CQDs maintained 90% of its original quantum yield in the subsequent spin-cast self-assembled films. The CQD films exhibited optically smooth surfaces (about $\lambda/30$) that were attributed by the close-packed electrostatic self-assembly. Optical gain measurements based on amplified spontaneous emission (ASE) of these planar films, which were used in the present work as companion reference material, have been reported by us to show a very low pump energy density threshold, less than 100 $\mu J/cm^2$, with an ultrashort optical pulsed source.[14] The optical gain in such films is dominated by the lowest bound electron-hole pair state, the single-exciton regime, with significant cross-section enhancement to optical gain. Question we answer here is whether such films could be deposited conformally on non-planar structures to fabricate laser-devices, such as grating structures where the groove depth was comparable to or exceeded the CQD solid film thickness.

Fig. 1a sketches our designed DFB laser structure where the high performance CQD gain media integrated with a second order DFB grating structure. This geometry is useful as it enables in-plane feedback for the laser (from the 2^{nd} order diffraction), and an output beam (from the 1^{st} order diffraction) perpendicular to the grating plane. The second order grating also eases the nanofabrication process because of the doubling of the grating period compared to a first order grating. Quartz gratings were made by laser interference holographic lithography, after numerical simulations which took into account the measured gain spectrum (from ASE

spectroscopy) and effective refraction index (n = 1.75 – 1.8) of the ~200 nm epitaxial-like $CdSe/Zn_{0.5}Cd_{0.5}S$ closely packed CQD films. After development of the photoresist in the holographic lithography process, the actual gratings were created in the quartz substrate by inductively-coupled-plasma reactive-ion-etching (ICP-RIE) using Chromium (Cr) as a hard mask.[21,22] After removing Cr, the gratings were cleaned by Piranha solution before the spin-casting process. Fig. 1b presents a cross sectional image of a typical quartz grating under scanning electron microscope (SEM), showing an almost vertical profile of the etched grating grooves. A densely packed CQD layer was deposited on top of the quartz grating by spin-casting technique to complete the CQD-DFB structure. Varying the concentration of CQD solution judiciously from 100 to 150 mg/ml, together with controlling the spinning speed from 1000 to 2500 RPM allowed us to control the film thickness from 100 to 500 nm. The SEM image of a cleaved CQD-DFB structure in Fig. 1c indicates that the densely packed CQD structure covers the entire grating grooves and forms an optically smooth top surface. Even under closer inspection, we do not find any significant deviations from conformal deposition of the CQD films, suggesting that the simple spin-casting method may be useful also for more complex contours in lasers and other types of light emitters. As an example beyond the DFB geometry, we have created CQD lasers with whispering gallery modes in spherical micro-resonator structures.[23] The packing density of the CQD film coated on DFB structures appears as high as that on planar surface (50%)[14]

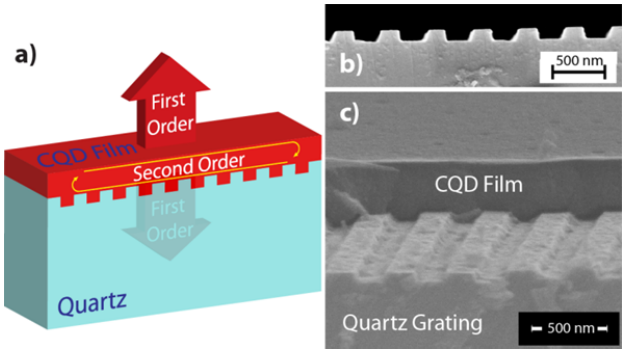

FIG. 1. Configuration of the second order DFB lasers with a dense CQD thin film as gain media. **(a)** Schematic of a CQD-DFB laser in which a 200 nm thick densely-packed CQD film is deposited on second order quartz grating. The pump beam direction is vertical (i.e. perpendicular to grating plane). The second order diffraction provides in-plane feedback for the CQD optical gain media while the first order diffraction provides two output coupling channels for the laser, each vertical (perpendicular) to the grating surface. **(b)** Cross-sectional SEM image of a quartz grating with a pitch of 400 nm. **(c)** An angled view of a complete CQD-DFB laser structure under SEM.

The CQD-DFB laser was pumped through a cylindrical lens in the similar stripe excitation configuration as the optical gain (ASE) characterization experiments on planar films[14] (spin-casted on flat surfaces). Note that the second order CQD-DFB laser emits vertically i. e. perpendicular to the grating's substrate surface while the ASE is from the edge and in the substrate plane. Fig. 2a-d present the summary data of the stripe-excited CQD-DFB laser at different pumping levels, showing the threshold behavior while transitioning to a laser action. When imaging the luminescence from the stripe region below the threshold excitation level, a uniform stripe (Fig. 2a) was expected from the normal spontaneous emission. Visually, above the threshold level, the intensity at the stripe center abruptly increased as seen in Fig. 2b and 2c until the entire stripe was strikingly bright (Fig. 2d). Notably, we used as optical pump source a

compact solid state laser (532 nm, 1 kHz, PowerChip laser from Teem Photonics) with a pulse duration (full with at half maximum, FWHM) τ_{pulse}= 270 ps, that is 2.25 times longer than the multiexciton Auger recombination time constant (τ_{Au} = 120 ps),[14] thus entering a regime of quasi-steady state. Unlike bulk semiconductor materials, non-radiative multiexciton Auger recombination process whose Coulomb-driven interaction is much enhanced in a strong confinement system.[24] Auger time constants in CdSe-based CQDs are about two orders faster than radiative recombination,[25,26] thwarting the population inversion building process. As a consequence, ultrafast or ultrahigh power pumping sources have been employed to overcome Auger losses in laser studies with biexciton gain mechanism in type-I CQDs. Type-II CQDs with their engineered core-shell structure were introduced to overcome multiexciton Auger losses by enabling single exciton gain,[27] but their cross sections of optical transition (proportional to gain) is significantly reduced due to minimal overlap of electron and hole wave functions, therefore, the ASE threshold is still relatively high. Seminally advantageous, the single exciton gain mechanism in our highly efficient type-I CQD films enables the quasi-CW DFB laser performance with significantly low thresholds as described next.

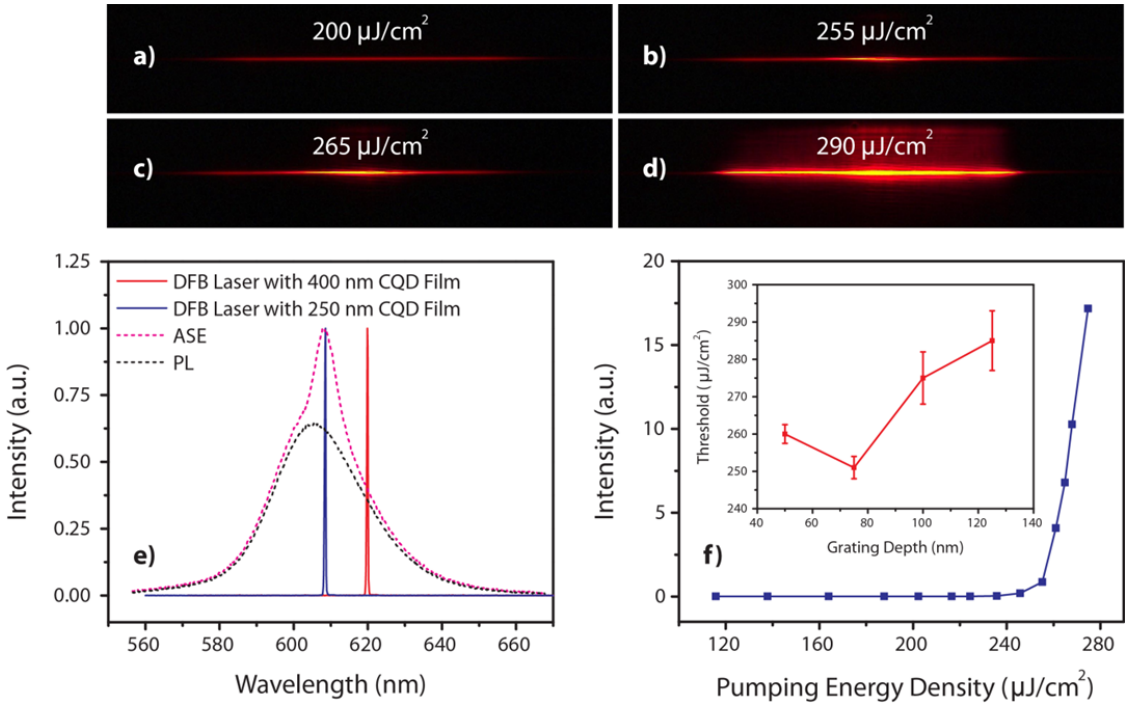

FIG. 2. Characteristics of the red CQD-DFB lasers and the CQD gain media. **Upper Panel: (a-d)** Plan view microphotographs of an excited stripe on a DFB structure at four different pulsed pump energy densities. The grating groove direction is perpendicular to the excitation stripe. **Lower Panels**: **(e)** Spectral analysis of the PL and ASE from a CQD thin film on a flat quartz substrate and single mode CQD-DFB lasers in which a single quartz grating was coated with a CQD layer of two different thicknesses. **(f)** Output intensity of single mode CQD-DFB laser as a function of pump pulse energy density demonstrates a threshold behavior. **Inset:** The threshold pump energy density of the CQD-DFB lasers as a function of quartz grating depth (H).

Fig. 2e presents the spectral analysis of the edge emission in stripe excitation of the planar CQD film spin-casted on flat quartz surface and the vertical emission of the second order CQD-DFB lasers. The edge emission of the planar CQD film shows a well-defined threshold behavior with

abruptly increasing in intensity and spectral narrowing. The emission changed from pure spontaneous emission (photoluminescence with peak of 604 nm and FWHM of 29 nm) to ASE (gain peak of 608 nm and FWHM of 8 nm) at the threshold of about 720 μJ/cm^2. The CQD films were also pumped by much longer optical pump pulses with wavelength of 532 nm and FWHM of 8 ns, comparable to spontaneous emission time constant. Aided by the single exciton gain mechanism, the ASE at this quasi-CW regime was achieved[23] at threshold of 1.75 mJ/cm^2. For two different CQD-DFB structures, clear single mode laser characteristics with a very narrow linewidth are evident (FWHM < 0.26 nm, limited by our spectrometer resolution.) In this example, a single quartz grating with the period P = 360 nm and groove depth H = 75 nm was used for CQD film deposition at different thicknesses. It is worth noting that the quartz gratings themselves are reusable for testing different CQD layers (or for other repeated, even applied uses) because the CQD films can be resolved off the grating by toluene solvent, and a subsequent Piranha solution can be employed to clean the quartz grating surface. The densely packed CQD films have an ellipsometrically measured refractive index of 1.75 – 1.8 at the wavelength of 632 nm[14], while the refractive index of quartz is 1.54. Controlling the CQD film thickness does change the effective refractive index of the entire CQD-DFB structure, even if slightly (on the order of $\Delta n/n \sim 10^{-2}$) and therefore "tunes" the laser wavelength as much as the net gain allows. A thicker (T = 400 nm) CQD film pulls the wave-guided mode more into the high refractive index material (CQD film) thereby increasing the effective refractive index of the entire optical structure and red-shifts the laser wavelength to 620 nm, which is spectrally detuned off the peak gain. By fine tuning the thickness of CQD film to approximately T = 250 nm, we could blue shift the CQD-DFB laser wavelength to the gain peak and thereby reduce the lasing pump threshold by factor of 5. Such a threshold reduction makes laser operation much more stable (and increases

longevity). Fig. 2f shows the laser intensity as a function of pumping energy density, demonstrating a clear threshold behavior for the case of a λ=608 nm CQD-DFB laser (T = 250 nm and H = 75 nm.) Here the threshold pump pulse energy density is 250 μJ/cm^2, in turn about 3 times lower than that for the threshold of ASE, a cavity-less laser. We infer from the corresponding ASE threshold that the CQD-DFB laser threshold with 8 ns optical pump pulse should be approximately 600 μJ/cm^2, an order lower than the values reported with CQD-DFB structures using 5 ns pulses at similar pump wavelength.[19] The thresholds here also present a practical pumping level, accessible with compact solid state lasers, few times less than that for type-I CQD biexciton gain[13,15,24,25] or type-II CQD single exciton gain[27] pumped by ultrashort pulsed sources. Note that, the CQD absorption coefficient at 400 nm wavelength of ultrashort pulse source is 5.5 times higher than that at our 532 nm pump wavelength. The inset in Fig. 2f presents the dependence of the CQD-DFB laser threshold on the groove depth, in which the different groove depth gratings were etched on a single Cr-masked quartz substrate, so as to reduce variation in their pitch. The optimized structure for lowest threshold is empirically found to be around H = 75 nm. We note that increasing the groove depth increases both the second order DFB grating mode (the cavity feedback) and the first order DFB grating mode (the cavity loss). These opposite effects make the lasing threshold less sensitive to groove depth around the optimum condition. The groove depth variation from 50 nm to 125 nm induces a laser wavelength change of about 2 nm, stable in the range of 8 nm FWHM gain spectrum.

With the optimized CQD-DFB laser, we demonstrate the spatial coherent outputs of the CQD-DFB lasers in Fig. 3. As noted, a second order DFB structure provides feedback only in one dimension (i.e. the in-plane stripe direction) in which the output beam is well collimated (unlike a conventional mesa edge emitting semiconductor laser) as seen in Fig. 3a. The top-view of the

CQD-DFB laser on Fig. 3b shows a robust emission under the bright room lighting. In this instance, the beam was emitted from the CQD-DFB laser with 200 μm long excitation stripe. However, we note that the stripe can be as short as 100 μm and below, thus approaching potential pixel dimensions e.g. in a high intensity display or projector. To define a circular beam, a second cylindrical lens was used to collimate the laser outputs in the vertical dimension as presented in Fig. 3c. A crisp laser spot on the target screen demonstrated an unambiguous presence of a spatially coherent CQD-DFB laser beam. The supplemental video (enhanced online) gives a laboratory view of the collimated beam with a well-defined beam spot at a remote target screen.

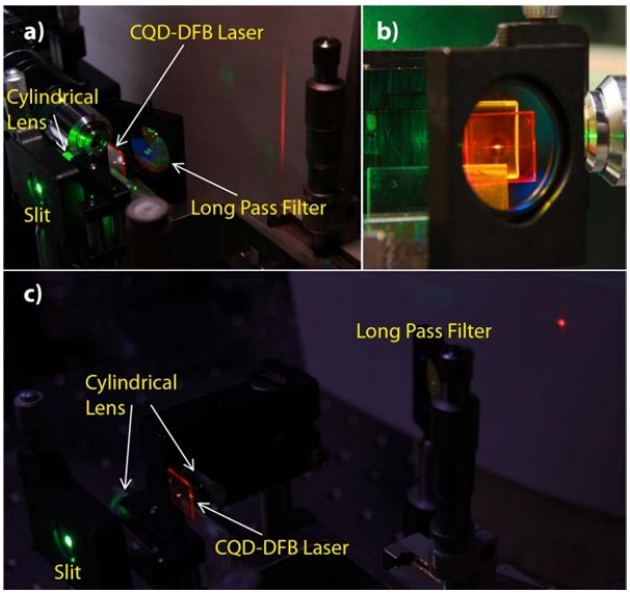

FIG. 3. Spatially coherent output beams from the red CQD-DFB lasers. **(a)** A strong laser output directly from a CQD-DFB laser stripe with dim room light. **(b)** Top view of the laser output in bright room light. **(c)** The circular beam from a single mode CQD-DFB laser where a second cylindrical lens was used to collimate the laser output, resulting in a well-defined laser spot on the screen. A long pass filter was used to remove residue green pumping beam; and a slit was used to control the excitation stripe length. The recored

movie in the laboratory illustrates the brightness, spatial coherent and well-collimated beam at the various distances from the laser source, (enhanced online).

In our present geometry, there are two output beams emerging perpendicular to each side of grating in opposite directions, respectively. We measured a total raw energy conversion efficiency of 7% for the CQD-DFB laser. However, since in the present experiments, about 75% of the pump beam power passed through the structure unabsorbed, the actual efficiency (output power vs. absorbed power) of the CQD-DFB laser is 28%, equivalent to the quantum efficiency (number of output laser photons vs. number of absorbed photons) of 32%, a welcome high performance level and, in turn, reaching into the regime of the single exciton quantum yield. We note that fundamentally, a biexciton-based system with fast nonradiative Auger recombination (2 orders faster than radiative recombination) simply cannot produce a laser at such high efficiency. Our maximum measured time-average of power was approximately 0.4 mW, which is somewhat akin to a red semiconductor laser pointer in terms of power as well as collimation and efficiency. We note that no effort whatsoever was spent in this DFB laser demonstration towards heat management or packaging. These first proof-of-concept CQD-DFB lasers presently last an hour before the onset of most probably heat induced degradation.

In conclusion, we have achieved a key step in transitioning CQDs towards possible practical lasers in the visible. Specifically, efficient second order CQD-DFB lasers in the red were implemented in a quasi-CW optically pumped regime while taking advantage of the fundamentally unique benefits of the single exciton gain regime which is now accessible in type-I CdSe/ZnCdS core/shell CQD materials. The CQD-DFB structure was optimized for high power, efficiency and spatially coherent collimated beam output. The approach is scalable and is

readily usable for any other visible colors with different sizes of CQDs, in particular the extension to the green and blue CQD-DFB lasers - based on a single material.

Acknowledgements

Financial support for this research was provided by the National Science Foundation under grant: ECCS-1128331 and Department of Energy (BES office) under grant: DE-FG02-07ER46387.

REFERENCES

[1] William Paul Risk, Timothy R. Gosnell, and Arto V. Nurmikko, *Compact blue-green lasers*. (Cambridge University Press, Cambridge, UK, 2003).

[2] C. B. Murray, D. J. Norris, and M. G. Bawendi, J. Am. Chem. Soc. **115**, 8706 (1993).

[3] L. E. Brus, J. Chem. Phys. **80** (9), 4403 (1984).

[4] Katherine Bourzac, Nature **493**, 283 (2013).

[5] Ute Resch-Genger, Markus Grabolle, Sara Cavaliere-Jaricot, Roland Nitschke, and Thomas Nann, Nat. Meth. **5** (9), 763 (2008).

[6] Igor L. Medintz, H. Tetsuo Uyeda, Ellen R. Goldman, and Hedi Mattoussi, Nat. Mater. **4** (6), 435 (2005).

[7] Qiang Zhang, Cuong Dang, Hayato Urabe, Jing Wang, Shouheng Sun, and Arto Nurmikko, Opt. Express **16** (24), 19592 (2008).

[8] Seth Coe-Sullivan, Wing-Keung Woo, Moungi Bawendi, and Vladimir Bulovic, Nature **420** (6917), 800 (2002).

[9] Cuong Dang, Joonhee Lee, Yu Zhang, Jung Han, Craig Breen, Jonathan S. Steckel, Seth Coe-Sullivan, and Arto Nurmikko, Adv. Mater. **24** (44), 5915 (2012).

[10] Yasuhiro Shirasaki, Geoffrey J. Supran, Moungi G. Bawendi, and Vladimir Bulovic, Nat. Photon. **7** (1), 13 (2013).

[11] Xuyong Yang, Dewei Zhao, Kheng Swee Leck, Swee Tiam Tan, Yu Xin Tang, Junliang Zhao, Hilmi Volkan Demir, and Xiao Wei Sun, Adv. Mater. **24** (30), 4180 (2012).

[12] Ryan R. Cooney, Samuel L. Sewall, D. M. Sagar, and Patanjali Kambhampati, Phys. Rev. Lett. **102** (12), 127404 (2009).

[13] V. I. Klimov, A. A. Mikhailovsky, Su Xu, A. Malko, J. A. Hollingsworth, C. A. Leatherdale, H.-J. Eisler, and M. G. Bawendi, Science **290** (5490), 314 (2000).

[14] Cuong Dang, Joonhee Lee, Craig Breen, Jonathan S. Steckel, Seth Coe-Sullivan, and Arto Nurmikko, Nat. Nanotechnol. **7** (5), 335 (2012).

[15] A. V. Malko, A. A. Mikhailovsky, M. A. Petruska, J. A. Hollingsworth, H. Htoon, M. G. Bawendi, and V. I. Klimov, Appl. Phys. Lett. **81** (7), 1303 (2002).

[16] Francesco Todescato, Ilaria Fortunati, Samuele Gardin, Eleonora Garbin, Elisabetta Collini, Renato Bozio, Jacek J. Jasieniak, Gioia Della Giustina, Giovanna Brusatin, Stefano Toffanin, and Raffaella Signorini, Adv. Funct. Mater. **22** (2), 337 (2012).

[17] Hans-Jurgen Eisler, Vikram C. Sundar, Moungi G. Bawendi, Michael Walsh, Henry I. Smith, and Victor Klimov, Appl. Phys. Lett. **80** (24), 4614 (2002).

[18] Shuai Gao, Chunfeng Zhang, Yanjun Liu, Huaipeng Su, Lai Wei, Tony Huang, Nicholas Dellas, Shuzhen Shang, Suzanne E. Mohney, Jingkang Wang, and Jian Xu, Opt. Express **19** (6), 5528 (2011).

[19] Yujie Chen, Benoit Guilhabert, Johannes Herrnsdorf, Yanfeng Zhang, Allan R. Mackintosh, Richard A. Pethrick, Erdan Gu, Nicolas Laurand, and Martin D. Dawson, Appl. Phys. Lett. **99** (24), 241103 (2011).

[20] O. Goede, L. John, and D. Hennig, Phys. Status Solidi (b) **89** (2), K183 (1978).

[21] Joonhee Lee, Sungmo Ahn, Hojun Chang, Jaehoon Kim, Yeonsang Park, and Heonsu Jeon, Opt. Express **17** (25), 22535 (2009).

[22] Joonhee Lee, Sungmo Ahn, Sihan Kim, Dong-Uk Kim, Heonsu Jeon, Seung-Jae Lee, and Jong Hyeob Baek, Appl. Phys. Lett. **94** (10), 101105 (2009).

[23] See supplementary material at [URL will be inserted by AIP] for a colloidal quantum dot whispering gallery mode laser in a spherical micro-resonator and the ASE threshold with 8 ns optical pump pulses.

[24] Samuel L. Sewall, Ryan R. Cooney, Eva A. Dias, Pooja Tyagi, and Patanjali Kambhampati, Phys. Rev. B **84** (23), 235304 (2011).

[25] Brent Fisher, Jean-Michel Caruge, Yin-Thai Chan, Jonathan Halpert, and Moungi G. Bawendi, Chem. Phys. **318** (1-2), 71 (2005).

[26] V. I. Klimov, A. A. Mikhailovsky, D. W. McBranch, C. A. Leatherdale, and M. G. Bawendi, Science **287**, 1011 (2000).

[27] Victor I. Klimov, Sergei A. Ivanov, Jagjit Nanda, Marc Achermann, Ilya Bezel, John A. McGuire, and Andrei Piryatinski, Nature **447** (7143), 441 (2007).